

Neutron Scattering Studies of Pyrochlore Compound $\text{Nd}_2\text{Mo}_2\text{O}_7$ in Magnetic Field

Yukio Yasui¹, Satoshi Iikubo¹, Hiroshi Harashina¹, Taketomo Kageyama¹, Masafumi Ito¹ Masatoshi Sato¹ and Kazuhisa Kakurai²

¹Department of Physics, Division of Material Science, Nagoya University,
Furo-cho, Chikusa-ku, Nagoya 464-8602

²Advanced Science Research Center, Japan Atomic Energy Research Institute, Tokai-mura, Naka-gun,
Ibaraki, 319-1195

Abstract

Neutron diffraction studies have been carried out in the applied magnetic field $\mathbf{H} // [0\bar{1}1]$ on a single crystal of pyrochlore ferromagnet $\text{Nd}_2\text{Mo}_2\text{O}_7$, whose Hall resistivity (ρ_H) has been reported to have quite unusual magnetic field (\mathbf{H})- and temperature (T)- dependences. The intensities of the observed magnetic reflections have been reproduced at 1.6 K as a function of H , by considering the change of the magnetic structure with H , where effects of the exchange fields at the Mo and Nd sites induced by the Mo-Mo and Mo-Nd exchange interactions and the single ion anisotropies of Mo³⁺ and Nd³⁺ moments are considered. From the H -dependent magnetic structure, the H -dependence of ρ_H has been calculated by using the chiral order mechanism. By comparing the result with the H -dependence of the observed ρ_H , it is found that the chiral order mechanism does not work well in the present system.

corresponding author : M. Sato (e-mail: msato@b-lab.phys.nagoya-u.ac.jp)

Keywords: pyrochlore molybdate, neutron scattering, magnetic structure,
spin chirality, anomalous Hall resistivity

Introduction

Pyrochlore molybdate $R_2Mo_2O_7$ ($R=Y$ and various rare earth elements) belongs to the pyrochlore series of compounds described by the general formula of $A_2B_2O_7$. The compounds have the face-centered cubic structure with the space group $Fd\bar{3}m$, in which A, B, O(1) and O(2) atoms fully occupy the sites 16d(A), 16c(B), 48f(O(1)) and 8b(O(2)), and the former two individually form three dimensional networks of corner-sharing tetrahedra.¹⁾ The local principal axis of a corner site of a tetrahedron corresponds to the line which connects the site with the center of gravity of the tetrahedron. Because the single ion anisotropy of magnetic moments determined by the symmetry of local arrangement of surrounding atoms directs along the principal axis and because there are four different but crystallographically equivalent principal axes corresponding to the four corner sites, along [111] and other directions, non-collinear or non-coplanar magnetic structure is often expected.

In $R_2Mo_2O_7$, both the transport and the magnetic properties seem to exhibit systematic variation with the ionic radius of R^{3+} , that is, for the relatively larger elements $R=Nd, Sm$ and Gd , the system exhibits the ferromagnetic transition, whereas for the smaller $R=Tb-Lu$ and Y , it is insulating and exhibits the spin-glass-like behavior.²⁻⁴⁾ The spin-glass behavior is considered to originate from the geometrical frustration

$Nd_2Mo_2O_7$ is metallic and exhibits a ferromagnetic transition at a Curie temperature $T_C=93$ K. Neutron diffraction studies on a single crystal of $Nd_2Mo_2O_7$ were carried out and the magnetic structure in the temperature(T) region of $4\text{ K} \leq T \leq T_C$ has been proposed by the authors' group in refs. 5 and 6. In the T region between 30 K and T_C , the ferromagnetic ordering at $T_C=93$ K is primarily associated with the Mo-moments, while the ordering of the Nd moments becomes significant below 30K. The net magnetization of the Nd-moments is antiparallel to that of the Mo-moments. The low temperature magnetic structure is non-collinear for both the Mo- and Nd-moments: The Mo-moments align along the direction nearly parallel to the [001] or other equivalent axes, but slightly tilted towards the local principal axes, while the Nd moments are along the directions almost parallel to their principal axes with their net magnetization being antiparallel to that of the Mo-moments. Because two of four Nd moments at corner sites of a tetrahedron direct inwards and the other two direct outwards of the tetrahedron, the magnetic structure is called "two-in and two-out" configuration.

Unusual behavior of the Hall resistivity (ρ_H) on single crystals of $Nd_2Mo_2O_7$ in the magnetic field (H) along [111] or [001] direction has been reported by the authors' group.^{7,8)} In the T region of $30\text{ K} < T < T_C$, where the net magnetization is primarily from the Mo-moments, H -dependence of the Hall resistivity can be described by the well-known equation $\rho_H=R_0H+4\pi R_sM$ as for ordinary ferromagnets, where R_0 and R_s are the ordinary and anomalous Hall coefficients, respectively, and M is the total magnetization. In the temperature region of $T < 30$ K, where the ordering of the Nd-moments is significant, the expression no more works and instead, another phenomenological equation $\rho_H=R_0H+4\pi R_sM_{Mo}+4\pi R'_sM_{Nd}$ has been found to describe the experimental results rather well, where M_{Mo} and M_{Nd} , and R_s and R'_s are the net magnetizations and the anomalous Hall coefficient which correspond to the Mo- and Nd-moments, respectively. $R_s \times R'_s$ is found to be negative. (We defined the sign of M_{Nd} to be negative if M_{Nd} is antiparallel to M_{Mo} .) It is interesting that R_s and R'_s do not exhibit significant decrease as T approaches zero, which is rather different from the behavior of the ordinary ferromagnets.^{9,10)} Although many

theoretical works have been reported on the anomalous Hall effect, old theories which are based on the band picture¹¹⁾ or on the mechanism of the conduction electron scattering by localized moments¹²⁾, cannot describe this behavior. Effects of the Ti-doping into the Mo sites on the Hall resistivity have also been studied on single crystals of the present system, where it is found that the sign change of R_s takes place with the small amount of the Ti-doping with the sign of R_s unchanged.¹³⁾ This indicates that two components are necessary to describe the behavior of ρ_H of $\text{Nd}_2\text{Mo}_2\text{O}_7$.

A new proposal has been made that the ordering of the spin chirality(χ) contributes to the Hall resistivity, where χ is locally defined as $\chi \equiv \mathbf{S}_1 \cdot \mathbf{S}_2 \times \mathbf{S}_3$ for three spins \mathbf{S}_1 , \mathbf{S}_2 and \mathbf{S}_3 .¹⁴⁾ In this theory, the anomalous Hall conductivity $\sigma_H (= \rho_H / \rho^2)$ is proportional to the fictitious magnetic flux(Φ) induced by the spin chirality χ , where ρ is the electrical resistivity. Taguchi *et al.* proposed that the spin chirality or the fictitious magnetic flux of the Mo-moments is playing an important role in determining the unusual behavior of the Hall resistivity.¹⁵⁾ However, authors' group has reported that the idea does not seem to consistently explain the observed behavior.^{5,6,13)} It is important for clarifying the relationship between the spin chiral order and the anomalous Hall resistivity, to study the detailed magnetic structure of $\text{Nd}_2\text{Mo}_2\text{O}_7$, particularly to study the magnetic structure in the applied magnetic field.

In the present work, neutron scattering studies have been carried out on a single crystal of $\text{Nd}_2\text{Mo}_2\text{O}_7$ in the applied magnetic field $\mathbf{H} // [0\bar{1}1]$ up to 5.7 T. The H -dependence of the magnetic structure is naturally understood by considering the Mo-Mo and Mo-Nd exchange fields and the single ion anisotropies of the Mo- and Nd-moments. Then, the spin chirality and the fictitious magnetic flux have been calculated as a function of H at $T=1.6$ K and as a function of T at $H=0$. Comparing the Hall resistivity ρ_H deduced from the fictitious magnetic flux with the experimentally observed data, we have found that the unusual behavior of the Hall resistivity of $\text{Nd}_2\text{Mo}_2\text{O}_7$ cannot consistently be understood by the chiral order mechanism in the present system.

Experiments

A single crystal of $\text{Nd}_2\text{Mo}_2\text{O}_7$ with a volume of $\sim 0.3 \text{ cm}^3$ was grown by a floating zone (FZ) method in Ar atmosphere. The magnetization and the Hall resistivity were measured by using edge parts of the crystal. The crystal planes of the samples were determined by observing the X-ray or neutron diffraction lines. The magnetization M and the Hall resistivity ρ_H were measured as a function of H by using a SQUID magnetometer, as described in refs.7 and 8.

Neutron measurements were carried out by using the triple axis spectrometer HQR(T1-1) installed at the thermal guide of JRR-3M of JAERI in Tokai, where the double axis condition was adopted. The crystal was oriented with the $[0\bar{1}1]$ direction vertical, where the $[011]$ and $[100]$ axes are in the scattering plane. The magnetic field was applied by using a superconducting magnet along the vertical or $[0\bar{1}1]$ direction. The 002 reflections of Pyrolytic graphite (PG) were used for both the monochromator and analyzer. Horizontal collimations were $12'$ (effective)- $20'$ - $60'$ and the neutron wavelength was 2.460 \AA . A PG filter was put in front of the sample to suppress the higher-order contamination.

Experimental Results and Discussion

In the fields $H=0$ and 5 T, the neutron elastic scattering intensity has been measured on the single crystal of $\text{Nd}_2\text{Mo}_2\text{O}_7$ at various \mathbf{Q} -points in the reciprocal space including those with half integer values of h and $k(=l)$ at 113 K ($>T_C$) and 1.6 K ($<T_C$). No reflection has been detected at \mathbf{Q} -points except the nuclear Bragg points. The scattering intensities at several nuclear Bragg points increases with decreasing T through the Curie temperature. The intensities also depend on the values of the external magnetic field H applied along $//[0\bar{1}1]$. Examples of the observed profiles of several reflections are shown in Figs. 1(a)-1(d), where the data at 113 K ($>T_C$) are the contribution from the nuclear reflection. In the present experiment, we have not observed the 002 nuclear reflection and all the nuclear reflections can be explained by the undistorted pyrochlore structure (space group $Fd\bar{3}m$). The observation of the reflection in the previous measurements^{5,6} is considered to be due to the imperfect removal of the high-order contamination. (The same crystal was used in the present and previous studies.) The profile widths of all reflections observed at 1.6 K under the magnetic field are equal to those of the instrumental resolution within the experimental error bars.

The magnetic scattering intensities I_{mag} of $\text{Nd}_2\text{Mo}_2\text{O}_7$ of the 111, 200, 022, 311 and 400 reflections are shown at 1.6K against the magnetic field $H(\mathbf{H}/[0\bar{1}1])$ in Figs. 2(a)-2(e), respectively, where the data are taken by scanning H stepwise up to 5.7 T after zero field cooling and then to zero. Hysteretic behavior of the $I_{\text{mag}}-H$ curves has been observed in the region of $H \leq 1.5$ T. It is due to the hysteretic domain motion. I_{mag} was obtained by taking the differences between the integrated intensities below and above T_C , where the absorption- and Lorentz factor-corrections were considered. The extinction effect has been estimated by plotting the observed values of the absolute structure factors $|F(\mathbf{Q})|^2$ of the nuclear scattering determined at 113K against those estimated by adopting the positional parameter $z = 0.333$ for 48f(O(1)) sites. Details of the extinction correction have already been reported in ref. 5. Effects of the error of the extinction correction do not bring about essential changes of the results of the present study, because only the data at the Bragg points where the extinction effect is not serious (or scattering intensity is relatively weak) are mainly considered in the magnetic structure analysis.

The system has the f.c.c. unit cell and the crystal structure consists of two networks individually formed by corner sharing tetrahedra of Mo_4 or Nd_4 as mentioned above. In this f.c.c. cell, each one of four primitive cells has a structure unit consisting of a Mo_4 -tetrahedron and a Nd_4 -one. In the measurements at 1.6 K in the zero- and finite magnetic fields, the magnetic reflections have been observed only at \mathbf{Q} -points with even h and k or odd h and k , where h and k are defined with respect to the f.c.c. unit cell. This result indicates that the magnetic primitive cell of $\text{Nd}_2\text{Mo}_2\text{O}_7$ has the same size as the chemical primitive cell. Then, to determine the magnetic structure of the present system, we are just required to find the moment arrangements within each one of Mo_4 - and Nd_4 -tetrahedra (or within a magnetic primitive cell).

First, we present the data taken at 1.6 K in zero magnetic field. The ordering patterns which can reproduce the intensity distribution of I_{mag} are shown for the Mo_4 - and Nd_4 - tetrahedra in Figs. 3(a) and 3(b), respectively, where thick arrows indicate the directions of the magnetic moments and G indicates the center of gravity of the tetrahedron. The net magnetizations M_{Nd} and M_{Mo} are along the $[001]$ or other equivalent directions (We have chosen this to be the $[001]$ direction (z axis) in Figs. 3(a) and 3(b).). The intensity distribution of I_{mag} calculated for the pattern is listed in Table I. In the calculation, we

used the reported values of the magnetic form factors for Nd³⁺ moments,¹⁶⁾ and for Mo⁴⁺, values experimentally determined for MoF₃ were used.¹⁷⁾ The distribution probability of the ferromagnetic domains among the three equivalent magnetization directions, [001], [010] and [100] is optimized.

The Mo-moments align along the direction nearly parallel to the *z* axis but have the slight tilting by the angle $\alpha = 4(\pm 4)^\circ$ from the *z* axis towards the corresponding local principal axes. The Nd-moments are along the directions nearly parallel to their principal axes with their *z*-component being antiparallel to the *z* axis, but the possibility of the tilting by $\pm 3^\circ$ from their principal axes cannot be excluded. The results indicate that there exists the relatively strong axial anisotropy at the Nd sites. The obtained magnetic ordering pattern indicates that the Mo-Mo and Mo-Nd interactions are ferromagnetic and antiferromagnetic, respectively. The values of the ordered atomic moments of Mo and Nd, μ_{Mo} and μ_{Nd} , respectively, are estimated by comparing the magnetic scattering intensities with the nuclear ones, to be about $1.30(\pm 0.05) \mu_{\text{B}}$ and $1.71(\pm 0.05) \mu_{\text{B}}$. The proposed ordering pattern does not contradict the pattern at 4.0 K reported in refs. 5 and 6. In the temperature region of $T \leq 30$ K, it is considered that μ_{Mo} is almost *T*-independent and μ_{Nd} increases with decreasing *T*. Considering the local arrangement of the Nd-moments which surround a Mo site, we expect that the ordered Mo-moments are tilted by the Mo-Nd antiferromagnetic exchange interaction towards the direction opposite to the local principal one. Then, with decreasing *T*, the values of α is expected to decrease.

Now, the ordering pattern of Nd₂Mo₂O₇ in the external magnetic field $\mathbf{H} // [0\bar{1}1]$ is discussed. The direction of the ordered Mo-moment at the *i*-th site, $\boldsymbol{\mu}_{\text{Mo},i}$ (The indices *i*(=1-4) indicate the four corner sites within a tetrahedron as shown in Figs. 5(a) and 5(b).) can be determined by the relation

$$\boldsymbol{\mu}_{\text{Mo},i} // (\mathbf{H} + \mathbf{H}_{\text{Mo} \leftarrow \text{Mo}} + \mathbf{H}_{\text{Mo} \leftarrow \text{Nd},i} + \mathbf{H}_{\text{ani}}^{\text{Mo}}) \quad (1)$$

where $\mathbf{H}_{\text{Mo} \leftarrow \text{Mo}}$ and $\mathbf{H}_{\text{Mo} \leftarrow \text{Nd},i}$ are the exchange fields from the surrounding Mo- and Nd-moments, respectively. $\mathbf{H}_{\text{ani}}^{\text{Mo}}$ is the effective magnetic field which describes the effect of the single ion anisotropy at the Mo-sites. The absolute value of $\boldsymbol{\mu}_{\text{Mo},i}$ at 1.6 K is equal to be $1.30 \mu_{\text{B}}$ and is considered to be *H*-independent. The absolute value of $\mathbf{H}_{\text{Mo} \leftarrow \text{Mo}}$ is estimated from the value of the Curie temperature $T_{\text{C}}=93$ K, which is primarily due to the ordering of the Mo-moments, is to be ~ 67 T. The direction of the ordered Nd-moment at the *j*-th site(*j*=1-4), $\boldsymbol{\mu}_{\text{Nd},j}$ is fixed along the [111] or other equivalent directions, by considering that the Nd-moments are in the doublet levels and have the strong Ising-like anisotropy, where the absolute value of the ordered Nd-moment, $\mu_{\text{Nd},j}$ can be described by the equations,

$$\mu_{\text{Nd},j}(T) = \mu_{\text{Nd},j}(T=0) \cdot \tanh \left(\frac{\boldsymbol{\mu}_{\text{Nd},j}(T=0) \cdot (\mathbf{H}_{\text{Nd} \leftarrow \text{Mo},j} - \mathbf{H})}{k_{\text{B}} T} \right) \quad (2)$$

where $\mathbf{H}_{\text{Nd} \leftarrow \text{Mo},j}$ is the exchange field at the *j*-th Nd site from the surrounding Mo-moments. Because the Weiss temperatures of Nd₂Zr₂O₇ and Nd₂GaSbO₇, which have the Nd-Nd atomic distances similar to that of Nd₂Mo₂O₇, is smaller than 1 K^{18,19)}, we expect that the interaction among the Nd-moments in Nd₂Mo₂O₇ is considered to be negligible. The absolute value of the ordered moment of Nd, $\mu_{\text{Nd},j}$ at *T*=1.6

K is equal to be $1.71 \mu_B$. $\mathbf{H}_{\text{Mo} \leftarrow \text{Nd}, i}$ and $\mathbf{H}_{\text{Nd} \leftarrow \text{Mo}, j}$ can be described by the equations as,

$$\mathbf{H}_{\text{Mo} \leftarrow \text{Nd}, i} = J_{\text{Mo-Nd}} \sum_j \boldsymbol{\mu}_{\text{Nd}, j}(T) \quad (3)$$

$$\mathbf{H}_{\text{Nd} \leftarrow \text{Mo}, j} = J_{\text{Mo-Nd}} \sum_i \boldsymbol{\mu}_{\text{Mo}, i}(T) \quad (4)$$

where $J_{\text{Mo-Nd}}$ is the coupling constant between the Mo- and Nd-moments and the summations are taken over the nearest neighbor sites. The dipole-dipole interaction between the Mo- and Nd-moments is of the order of 0.1 K and can be neglected here. Schematic figures of the directions of these fields at the Mo- and Nd-sites are shown in Figs. 4(a) and 4(b), respectively. We have chosen the values of $\mu_{\text{Nd}, j}(T=0)$, $J_{\text{Mo-Nd}}$ and $H_{\text{ani}}^{\text{Mo}}$ to reproduce the I_{mag} data obtained at the Bragg points listed in Table I and to reproduce the H -dependence of I_{mag} shown in Figs. 2(a)-2(e), where I_{mag} is scaled by the nuclear scattering intensities: $\mu_{\text{Nd}, j}(T=0)=1.93 \mu_B$, $J_{\text{Mo-Nd}}=-0.39 \text{ T}/\mu_B$ and $H_{\text{ani}}^{\text{Mo}}=7.6 \text{ T}$.

Once these values are determined, we can derive the magnetic structure of the present system for arbitrary \mathbf{H} and T . The obtained ordering patterns at 1.6 K in the magnetic field $H \rightarrow 0$ and $H=5.7 \text{ T}$ are shown in Figs. 5(a) and 5(b), respectively, where $H \rightarrow 0$ indicates that the magnetic field is extrapolated to zero from the relatively high magnetic field, and that the direction of the ferromagnetic component is uniquely given. The $\mu_{\text{Nd}, j}$ values ($j=1-4$) are shown against the magnetic field H at 1.6 K in Fig. 5(c). I_{mag} calculated for these patterns are shown against H in Figs. 2(a)-2(e) by solid lines. In the calculation, the intensity average has been taken for crystallographically equivalent Bragg points in the scattering plane, the plane perpendicular to H , to consider the degrees of freedom of the domain structure about the direction of \mathbf{H} . The Mo-moments align along the direction nearly parallel to $\mathbf{H}/[0\bar{1}1]$, but they are tilted from $[0\bar{1}1]$ direction by the $H_{\text{ani}}^{\text{Mo}}$ and $\mathbf{H}_{\text{Mo} \leftarrow \text{Nd}, i}$, with their tilting directions and angles depending on H through H -dependence of the magnitude of $\mu_{\text{Nd}, j}(T)$. The directions of $\mu_{\text{Nd}, j}$ ($j=1$ and 3) are nearly H -independent as shown in Figs. 5(a) and 5(b), because their directions (parallel to the corresponding principal axes) are perpendicular to \mathbf{H} and nearly perpendicular to $\mathbf{H}_{\text{Nd} \leftarrow \text{Mo}, j}$. The values of the ordered Nd-moment $\mu_{\text{Nd}, j}$ ($j=2$ and 4) turn out, as shown in Fig. 5(c), to become zero at $H=3.0 \text{ T}$, which can be considered to correspond to $H_{\text{Nd} \leftarrow \text{Mo}, j}$.

In Fig. 6, the M - H curves of a single crystal of $\text{Nd}_2\text{Mo}_2\text{O}_7$ taken at various temperatures after the zero field cooling under the field $\mathbf{H}/[0\bar{1}1]$ (or equivalently $\mathbf{H}/[110]$), is shown together with those calculated at 1.6 K and 3.0 K for the magnetic structure proposed above. We have found that the calculated data is quantitatively consistent with the experimentally observed data, though the difference is observed in the H -region of $H \leq 1 \text{ T}$, which arises from the fact that the calculated results are obtained for the magnetic state with the ferromagnetic component of all domains being aligned in the direction of H .

We have derived the magnetic structure of $\text{Nd}_2\text{Mo}_2\text{O}_7$ in the magnetic field $\mathbf{H}/[0\bar{1}1]$ by using the relations (1)-(4) and by using the values of $\mu_{\text{Nd}, j}(T=0)$, $J_{\text{Mo-Nd}}$ and $H_{\text{ani}}^{\text{Mo}}$ deduced from the experimental results. We have also derived the magnetic structures at 1.6 K under the conditions $\mathbf{H}/[001]$ and $[111]$ for the same values of $\mu_{\text{Nd}, j}(T=0)$, $J_{\text{Mo-Nd}}$ and $H_{\text{ani}}^{\text{Mo}}$ as those used above. We have further tried to determine the magnetic structures by using $H_{\text{ani}}^{\text{Mo}}=0$ instead of $H_{\text{ani}}^{\text{Mo}}=7.6 \text{ T}$, with

keeping $\mu_{Nd,j}(T=0)$ and J_{Mo-Nd} unchanged, though the degree of agreement between the calculated and the observed I_{mag} distributions for $H_{ani}^{Mo}=0$ is slightly worse than that for $H_{ani}^{Mo}=7.6$ T.

In the above calculations, the rather strong Ising-like anisotropy of the Nd moments is essential to reproduce the observed H -dependence of the magnetic scattering intensities, where the ordered Nd moment at $T=0$ $\mu_{Nd,j}(T=0)$ is found to be smaller than the moment value $g\mu_B J$ of the free Nd³⁺ ions ($J=9/2$). To understand this results, we consider a doublet with the expectation values of the angular momentum component along the principal axis, $\pm|J'|$ ($J'<J$), where the strong anisotropy can be expected if the energies of the lowest excited states are much larger than $\mu_{Nd,j}(T=0) \cdot H$ and $k_B T$. The components of J perpendicular to the principal axis are considered not to have the ordering.

In Figs. 7(a)-7(c), the Hall resistivities ρ_H of a single crystal of Nd₂Mo₂O₇ are shown at various temperatures against the magnetic fields H applied along the [110], [001] and [111] directions, respectively.^{7,8,13} The authors' group reported that the H - and T -dependences of ρ_H of Nd₂Mo₂O₇ are quite unusual: The behaviors of ρ_H are markedly different between the T -regions above and below ~ 30 K. Because the total magnetization is determined by the sum of the net magnetizations M_{Mo} and M_{Nd} which have opposite signs in the weak field region, the enhancement of ρ_H cannot be reproduced by the expression $\rho_H=R_0 H+4\pi R_s M$. Instead, the phenomenological expression $\rho_H=R_0 H+4\pi R_s' M_{Mo}+4\pi R_s'' M_{Nd}$ has been, as stated above, found to reproduce the results rather well, indicating that the perturbative treatment is valid. However, any of the old theories cannot describe the T -dependence of the Hall resistivity ρ_H of Nd₂Mo₂O₇.

Ohgushi *et al.*¹³ and Taguchi *et al.*¹⁴ have proposed that the ordering of the spin chirality χ contributes to the Hall resistivity. According to this mechanism, the fictitious magnetic flux ϕ induced by the spin chirality χ acts on the electron motion in the same way as the real magnetic field, where ρ_H cannot be treated by the perturbation of the spin-orbit interaction. The absolute value of the fictitious flux, $|\phi_i|$ ($i=1-4$) is proportional to $\chi \equiv \mathbf{S}_j \cdot \mathbf{S}_k \times \mathbf{S}_l$, where $\{j, k, l\}$ being the i -th set of different numbers chosen in a cyclic way from 1-4 to specify the set of spins within a tetrahedron, and its direction is defined as shown in Fig. 8 for ϕ_1 for example. The total fictitious magnetic flux Φ of the system is vector sum of $\phi_1 \sim \phi_4$. The anomalous Hall conductivity $\sigma_H (= \rho_H / \rho^2)$ is proportional to the parallel component of Φ to the external magnetic field.

The fictitious magnetic flux of the Mo- and Nd-moments of Nd₂Mo₂O₇, Φ_{Mo} and Φ_{Nd} , respectively, has been calculated at 1.6 K as a function of H by using the H -dependent magnetic structure derived above. Their parallel components to the external magnetic field H , Φ_{Mo}'' and Φ_{Nd}'' , are shown in Figs. 9(a)-9(c), for the cases $H//[110]$, [001] and [111], respectively. In the figures, the results obtained for both $H_{ani}^{Mo}=7.6$ T and $H_{ani}^{Mo}=0$ are plotted (Note that Φ_{Nd}'' hardly depend on the value of H_{ani}^{Mo}). Because the electrical resistivity ρ of Nd₂Mo₂O₇ below ~ 60 K is almost T - and H -independent^{13,19} in the H -region of $H \leq 7$ T, the Hall conductivity $\sigma_H (= \rho_H / \rho^2)$ is nearly proportional to the Hall resistivity ρ_H . It should be also noted that ρ_H does not significantly depend on T below 3 K.¹³ Then, according to the chiral order mechanism, the H -dependences of Φ_{Mo}'' and Φ_{Nd}'' , at 1.6 K shown in Figs 9(a)-9(c) should agree with those of the Hall resistivity ρ_H observed at 3 K, which are shown in Figs. 7(a)-7(c), respectively. However, we cannot find the agreement in the figures: For $H//[001]$, for example, the observed ρ_H decreases monotonically with increasing H , while the calculated Φ_{Mo}'' for $H_{ani}^{Mo}=7.6$ T increases with increasing

H and $\Phi_{\text{Mo}}^{\prime\prime}$ for $H_{\text{ani}}^{\text{Mo}}=0$ does not exhibit the strong decreasing behavior. (We note here that the ordinary Hall resistivity is not significantly large and its consideration does not change the above arguments.) As stated above, the observed $\rho_{\text{H}}H$ curves can phenomenologically be described by using two degrees of freedom which contribute to the anomalous Hall resistivity $\rho_{\text{H}}^{13)}$: One is proportional to M_{Mo} and the other is proportional to M_{Nd} . However, it is difficult to explain the observed ρ_{H} data by the linear combination of the components of $\Phi_{\text{Mo}}^{\prime\prime}$ and $\Phi_{\text{Nd}}^{\prime\prime}$,

Now, the T -dependence of the fictitious magnetic flux of the Mo- and Nd-moments, $\Phi_{\text{Mo}}^{\prime\prime}$ and $\Phi_{\text{Nd}}^{\prime\prime}$ is discussed. We calculate the fictitious flux by assuming that even at $H=0$, both of Φ_{Mo} and Φ_{Nd} , are parallel to the [001], or the ferromagnetic domains are aligned. Figure 10(a) shows their absolute values at $H=0$ divided by the corresponding value at 1.6 K. In the calculation, the ordered Nd-moments $\mu_{\text{Nd},j}(T)$ has been estimated from the temperature dependence of the observed magnetic scattering intensity I_{mag} of the 111 reflection shown in the inset of Fig. 10(a). For $H_{\text{ani}}^{\text{Mo}}=7.6$ T, $\Phi_{\text{Mo}}^{\prime\prime}$ decreases with decreasing T in contrast to that at $H_{\text{ani}}^{\text{Mo}}=0$. Figure 10(b) shows the T -dependence of the Hall resistivity ρ_{H} of $\text{Nd}_2\text{Mo}_2\text{O}_7$ taken under the relatively weak magnetic field $H=0.5$ T along the [001] direction. Because at $H=0.5$ T, the magnetic domains are aligned but the magnetic structure is not significantly changed from that at $H=0$, the observed ρ_{H} can be compared with the above calculated results at $H=0$. We find, however, that the T -dependences of $\Phi_{\text{Mo}}^{\prime\prime}$ and $\Phi_{\text{Nd}}^{\prime\prime}$, are quite different from that of the observed Hall resistivity as shown in Figs. 10(a) and 10(b), irrespective of the choice of the value of $H_{\text{ani}}^{\text{Mo}}$. Thus, the T and H -dependences of the fictitious magnetic flux deduced from the proposed magnetic structure do not agree with that of the observed Hall resistivity ρ_{H} of $\text{Nd}_2\text{Mo}_2\text{O}_7$, indicating that unusual behavior of ρ_{H} is not explained only by the chiral order mechanism.

In the above calculations of the fictitious magnetic flux, we have estimated the ordered Nd-moments $\mu_{\text{Nd},j}$ by using the mean field approximation. The problem might remain whether the spin chirality or the fictitious magnetic flux defined by the local arrangement of moments could properly be obtained from this $\mu_{\text{Nd},j}$. For example, even in the case where $H_{\text{ani}}^{\text{Mo}}=0$ and $\mu_{\text{Nd},j}=0$, non-zero $\Phi_{\text{Mo}}^{\prime\prime}$ is induced through the exchange interaction of Mo- and Nd-moments, if only the Mo-moments are ferromagnetically ordered. However, the value of $\Phi_{\text{Mo}}^{\prime\prime}$ induced in the situation is too small (by a factor of $\sim 1/50$) to explain the ρ_{H} value observed in the region of $T > 40$ K. Then, it is very difficult to expect significant effects of the local fluctuation of the chirality to the behavior of ρ_{H} . The observed behavior of ρ_{H} of the present system cannot be understood by considering the chiral order as the main mechanism of the Hall transport.

In summary, we have shown the neutron scattering data taken for a single crystal of $\text{Nd}_2\text{Mo}_2\text{O}_7$ in the T -region from 1.6 K to 150 K ($>T_{\text{C}}$) and under the magnetic field up to 5.7 T applied along the $[0\bar{1}1]$ direction. The magnetic structure in the applied magnetic field $0 \leq H \leq 5.7$ T is derived by estimating the exchange coupling constant between the Mo- and Nd-moments and by considering the single ion anisotropies of each Mo- and Nd-moments. From the proposed magnetic structure, the fictitious magnetic flux of the Mo- and Nd-moments has been calculated as functions of T and H and compared with the observed data of the Hall resistivity ρ_{H} . The results indicate that the chiral order mechanism is not, at least, playing a main role in determining the observed behavior of ρ_{H} in the present system.

Acknowledgements

The authors thank Prof. Nagaosa of the University of Tokyo for stimulating discussion. They also thank the Neutron Scattering Laboratory of the Institute for Solid State Physics(NSL-ISSP) and Research Center for Nuclear Science and Technology(RCNST) of the University of Tokyo for the use of the instrument within the national user's program.

References

- 1) For example, M. A. Subramanian, G. Aravamudan and G. V. Subba Rao: *Prog. Solid State Chem.* **15** (1983) 55.
- 2) M. Sato, X. Yan and J. E. Greedan: *Z. anorg. allg. Chem.* **540/541** (1986) 177.
- 3) N. Ali, M. P. Hill, S. Labroo and J.E. Greedan: *J. Solid State Chem.* **83** (1989) 178.
- 4) T. Katsufuji, H. Y. Hwang and S. -W. Cheong: *Phys. Rev. Lett.* **84** (2000) 1998.
- 5) Y. Yasui, Y. Kondo, M. Kanada, M. Ito, H. Harashina, M. Sato and K. Kakurai: *J. Phys. Soc. Jpn.* **70** (2001) 284.
- 6) Y. Yasui, Y. Kondo, M. Kanada, M. Ito, H. Harashina, S. Iikubo, K. Oda, T. Kageyama, K. Murata, S. Yoshii, M. Sato, H. Okumura and K. Kakurai: *Proc. 1st Int. Symp. Advanced Science Reserch, Advances in Neutron Scattering Reserch, J. Phys. Soc. Jpn.* **70** (2001) suppl. A. p.100.
- 7) S. Yoshii, S. Iikubo, T. Kageyama, K. Oda, Y. Kondo, K. Murata and M. Sato: *J. Phys. Soc. Jpn.* **69** (2000) 3777.
- 8) S. Iikubo, S. Yoshii, T. Kageyama, K. Oda, Y. Kondo, K. Murata and M. Sato: *J. Phys. Soc. Jpn.* **70** (2001) 212.
- 9) J. -P. Jan: *Helv. Phys. Acta* **25** (1952) 677.
- 10) J. J. Rhyne: *Phys. Rev.* **172** (1968) 523.
- 11) R. Kurplus and J. M. Luttinger: *Phys. Rev.* **95** (1954) 1154.
- 12) J. Kondo: *Prog. Theor. Phys.* **27** (1962) 772.
- 13) T. Kageyama, S. Iikubo, S. Yoshii, Y. Kondo, M. Sato and Y. Iye: *J. Phys. Soc. Jpn.* **70** (2001) 3006.
- 14) K. Ohgushi, S. Murakami and N. Nagaosa: *Phys. Rev.* **B62** (2000) R6065.
- 15) Y. Taguchi Y. Oohara, H. Yoshizawa, N. Nagaosa and Y. Tokura: *Science* **291** (2001) 2573.
- 16) P. J. Brown: *International Tables for Crystallography*, ed. A. J. C. Wilson (Kluwer, Dordrecht, 1992) vol. C, Chap. 4.
- 17) M. K. Wilkinson, E. O. Wollan, H. R. Child and J. W. Cable: *Phys. Rev.* **121** (1961) 74.
- 18) H. W. J. Blote, R. F. Wielinga and W. J. Huiskamp: *Physica.* **43** (1969) 549.
- 19) S. Yoshii *et al.* unpublished data

Figure captions

- Fig. 1. Profiles of the ω -scans for 111, 200, 022 400 reflections taken under the magnetic field $\mathbf{H} // [0\bar{1}1]$ are shown in (a)-(d), respectively. The values of H and T are shown in the figures.
- Fig. 2. Magnetic field H ($\mathbf{H} // [0\bar{1}1]$) dependence of the magnetic scattering intensities of $\text{Nd}_2\text{Mo}_2\text{O}_7$ at 1.6 K is shown for 111, 200, 022, 311 and 400 reflections in (a)-(e), respectively, where the data were taken after zero field cooling by scanning H stepwise up to 5.7 T and then down to zero. Solid lines show the calculated magnetic scattering intensities for the magnetic ordering pattern derived here. See text for details.
- Fig. 3. The magnetic ordering patterns which can explain the observed magnetic scattering intensities of $\text{Nd}_2\text{Mo}_2\text{O}_7$ taken at $T=1.6$ K and $H=0$, are shown for the Mo_4^- and Nd_4^- tetrahedra in (a) and (b), respectively, where thick arrows indicate the directions of the magnetic moments. G indicates the center of gravity of the tetrahedra.
- Fig. 4. Schematic figure of the magnetic fields which act on the (a) Mo^- and (b) Nd^- moments. \mathbf{H} is the external magnetic field along $[0\bar{1}1]$ direction. $\mathbf{H}_{\text{ani}}^{\text{Mo}}$ and $\mathbf{H}_{\text{ani}}^{\text{Nd}}$ are the effective magnetic fields derived from the single-ion anisotropy of the Mo^- and Nd^- moments, respectively. $\mathbf{H}_{\text{Mo} \leftarrow \text{Mo}}$ and $\mathbf{H}_{\text{Mo} \leftarrow \text{Nd}, j}$ are the exchange fields at the i -th Mo site within a tetrahedron from the surrounding Mo^- and Nd^- moments, respectively. $\mathbf{H}_{\text{Mo} \leftarrow \text{Nd}, j}$ is the exchange field at the j -th Nd site within a tetrahedron from the surrounding Mo^- moments.
- Fig. 5. Magnetic ordering patterns of the Mo_4^- and Nd_4^- tetrahedra, which can explain the observed magnetic scattering intensities of $\text{Nd}_2\text{Mo}_2\text{O}_7$ taken at 1.6 K under the magnetic fields (a) $H \rightarrow 0$ and (b) 5.7 T, respectively. Thick and thin arrows indicate the directions of the magnetic moments and the external magnetic field $\mathbf{H} // [0\bar{1}1]$, respectively. The absolute value of the ordered Nd^- moments, $\mu_{\text{Nd}, j}$ ($j=1-4$) are shown at 1.6 K against the magnetic field $\mathbf{H} // [0\bar{1}1]$ in (c). See text for details.
- Fig. 6. Magnetization M of $\text{Nd}_2\text{Mo}_2\text{O}_7$ is shown at various temperatures against the magnetic field H applied along $[0\bar{1}1]$, where dotted and solid lines show the results of the calculations at 1.6 K and 3.0 K, respectively, for the magnetic ordering pattern derived here (See Figs. 5(a)-5(c)).
- Fig. 7. Hall resistivity ρ_{H} of $\text{Nd}_2\text{Mo}_2\text{O}_7$ is shown at various temperatures against the magnetic field H applied along (a) $[110]$, (b) $[001]$ and (c) $[111]$, respectively. The data in (b) and (c) were reported previously by authors' group.^{7,8,13)}
- Fig. 8. Schematic figure of the directions of the magnetic moments and the fictitious magnetic flux within a tetrahedron. The direction of the fictitious flux ϕ is perpendicular to the triangle found by the sites of three spins and its absolute value $|\phi|$ is proportional to their spin chirality χ . The total fictitious magnetic flux Φ is the sum of the four vectors of the fictitious flux, ϕ determined by the three magnetic moments periodically chosen among the four moments within a tetrahedron.
- Fig. 9. Calculated fictitious magnetic flux of the Mo^- and Nd^- moments along the external magnetic field, $\Phi_{\text{Mo}''}$ and $\Phi_{\text{Nd}''}$, respectively, is shown at 1.6 K against the magnetic fields H applied along (a) $[110]$, (b) $[001]$ and (c) $[111]$, where solid and long dashed lines are for the Mo^- moments in the case of $\mathbf{H}_{\text{ani}}^{\text{Mo}}=7.6$ T and $\mathbf{H}_{\text{ani}}^{\text{Mo}}=0$, respectively, and the dashed line is

for the Nd-moments.

Fig. 10. (a) Temperature dependence of the absolute values of the calculated fictitious magnetic flux of the Mo- and Nd-moments, Φ_{Mo} and Φ_{Nd} , respectively, is shown at $H=0$ (Both are parallel to [001]). The values are scaled by the data at 1.6 K. Inset shows the temperature dependence of the observed magnetic scattering intensity of the 111 reflection taken for a single crystal of $\text{Nd}_2\text{Mo}_2\text{O}_7$. (b) Temperature dependence of the Hall resistivity ρ_{H} of $\text{Nd}_2\text{Mo}_2\text{O}_7$ taken under the magnetic field $H=0.5$ T along the [001] direction. Broken lines are the guides for the eye.

Table. I. Integrated intensities of the magnetic scattering taken at 1.6 K under the zero external field are compared with those of the model calculations at several reflection points.

$T=1.6\text{K}, H=0$		
hkl	I_{obs}	I_{calc}^*
111	339.2 ± 22.4	318.3
200	116.7 ± 6.0	112.0
022	37.9 ± 3.9	37.0
311	58.2 ± 5.9	63.9
400	10.8 ± 4.1	10.2
133	36.2 ± 21.1	44.6
422	23.7 ± 10.4	26.8
511	32.3 ± 10.5	27.2
600	21.4 ± 1.5	21.4

* for $\mu_{\text{Mo}}=1.30\mu_{\text{B}}, \mu_{\text{Nd}}=1.71\mu_{\text{B}}$

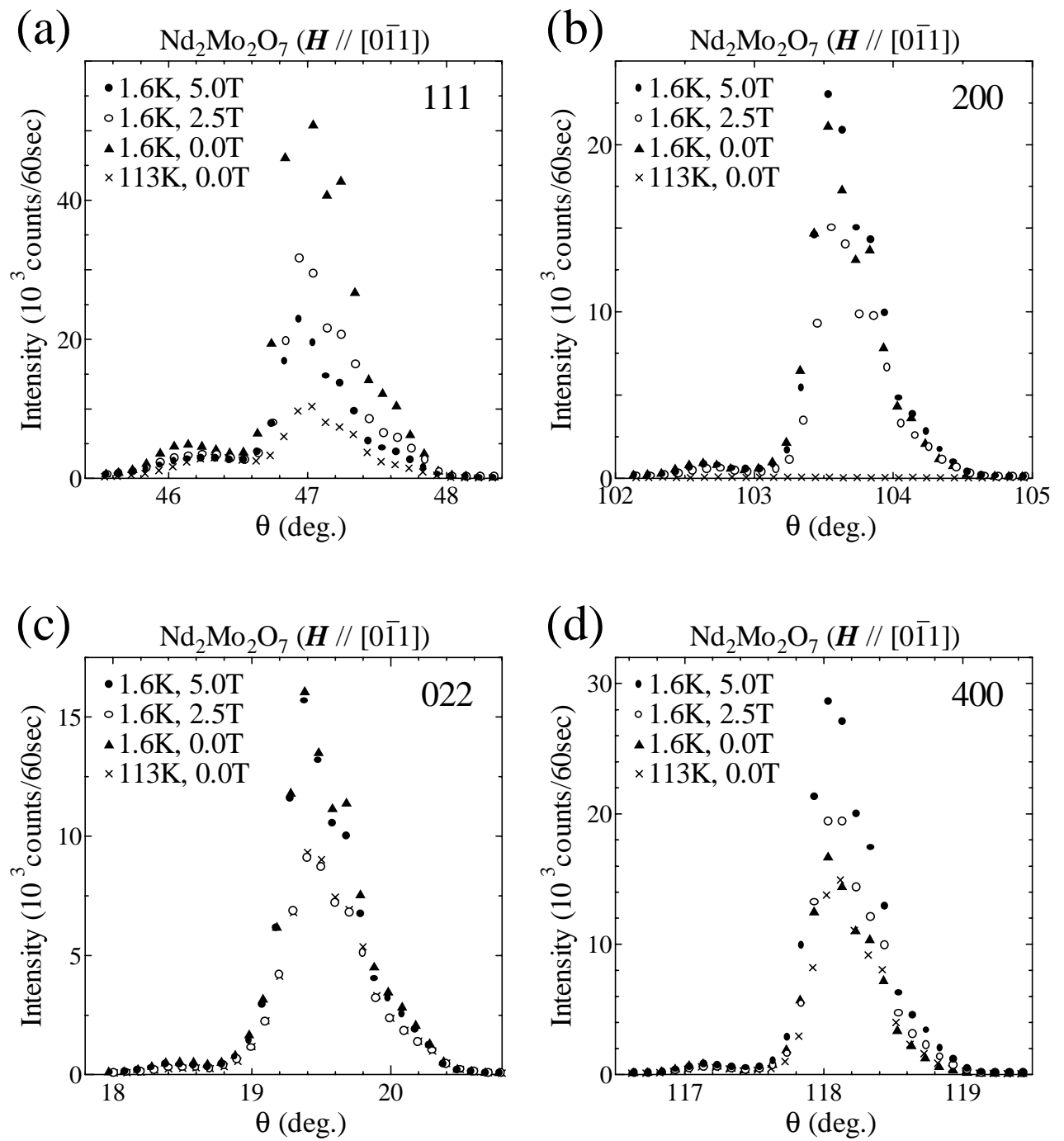


Fig. 1

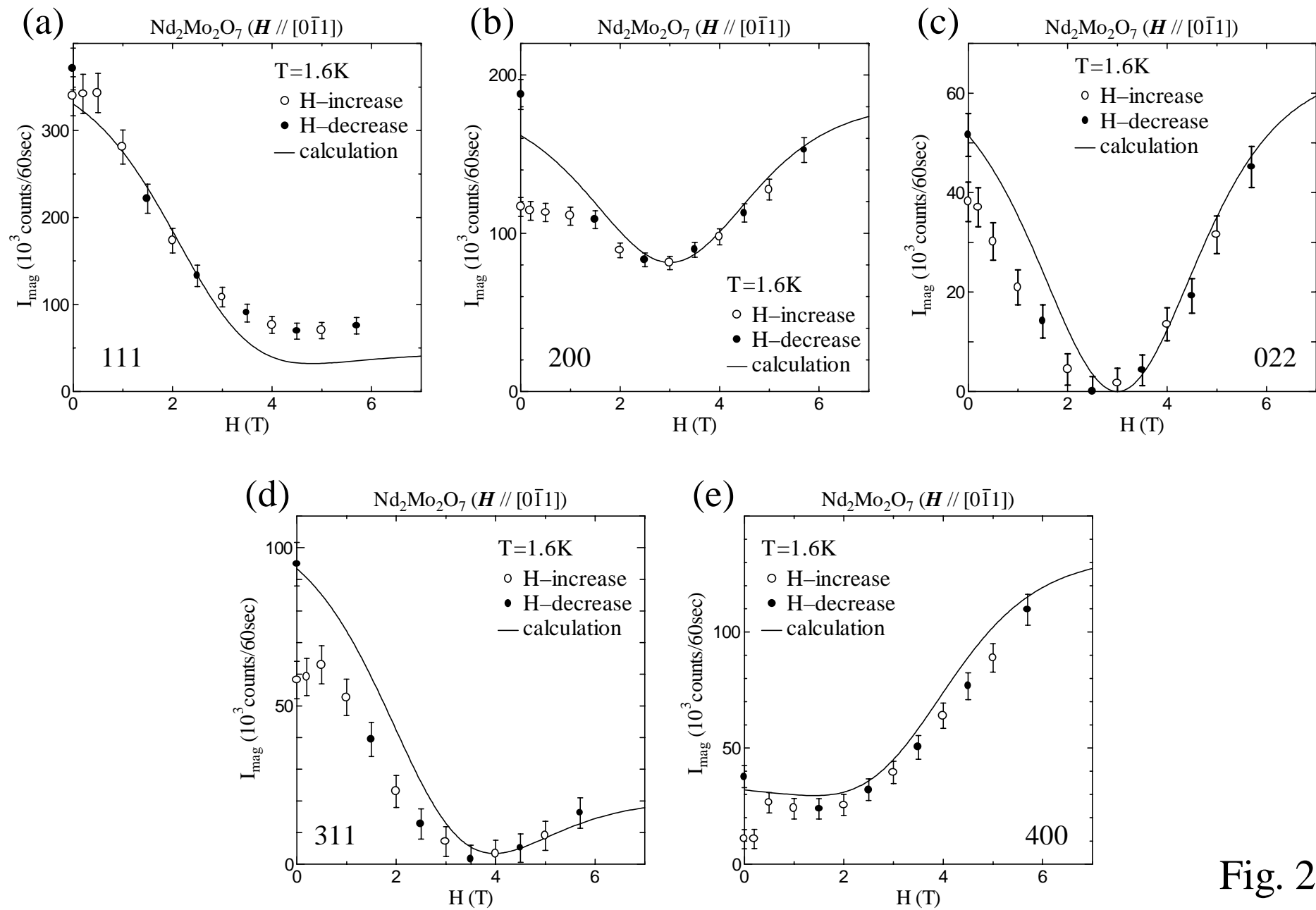


Fig. 2

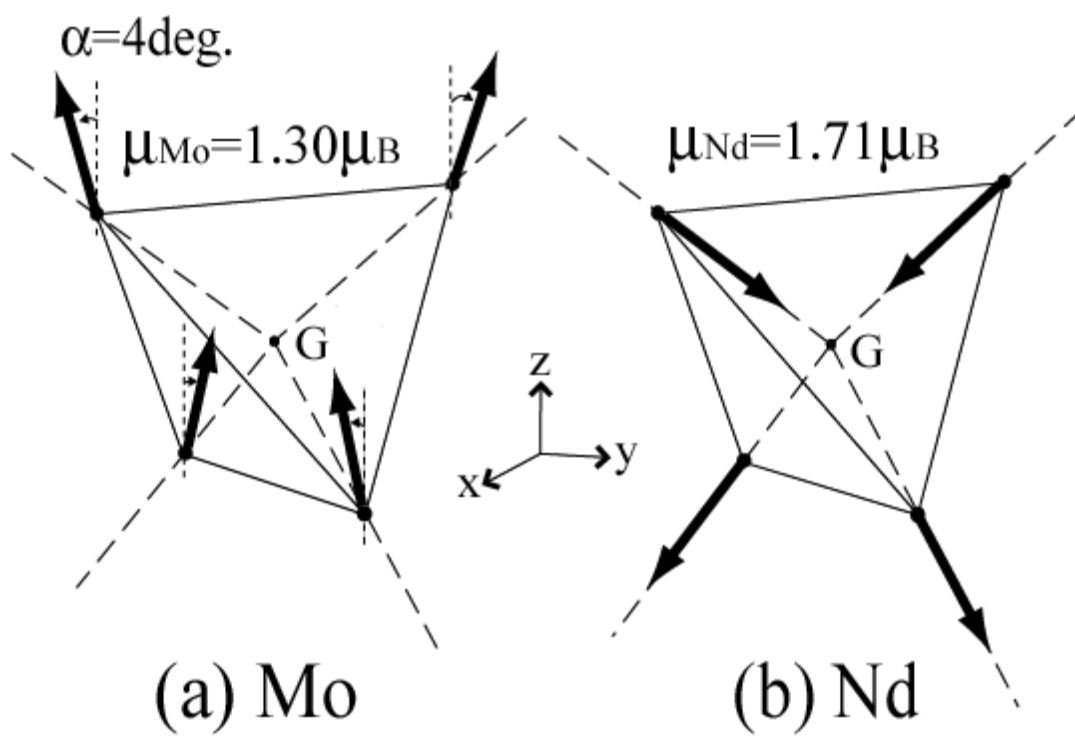


Fig. 3

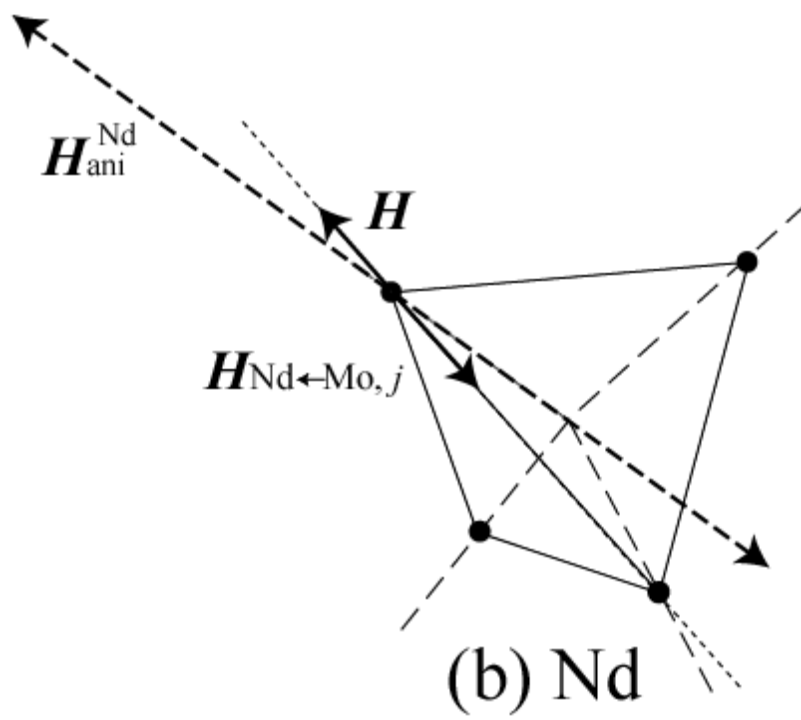
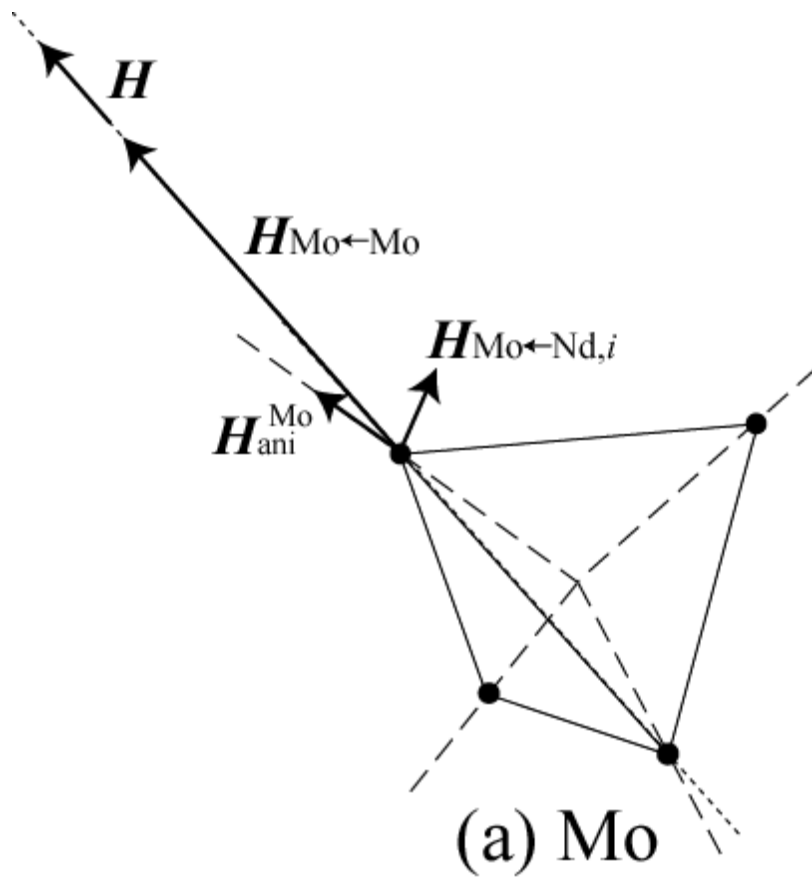
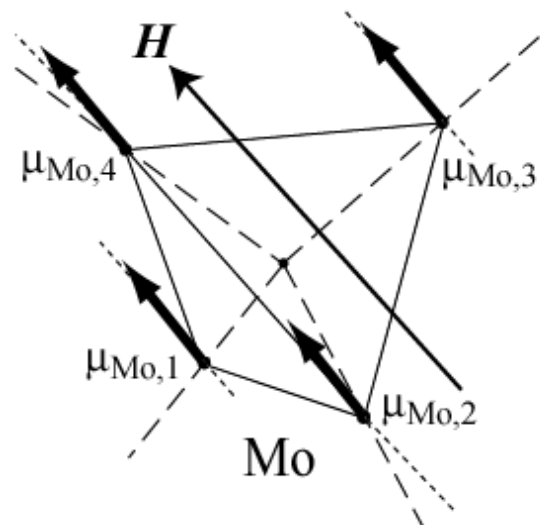
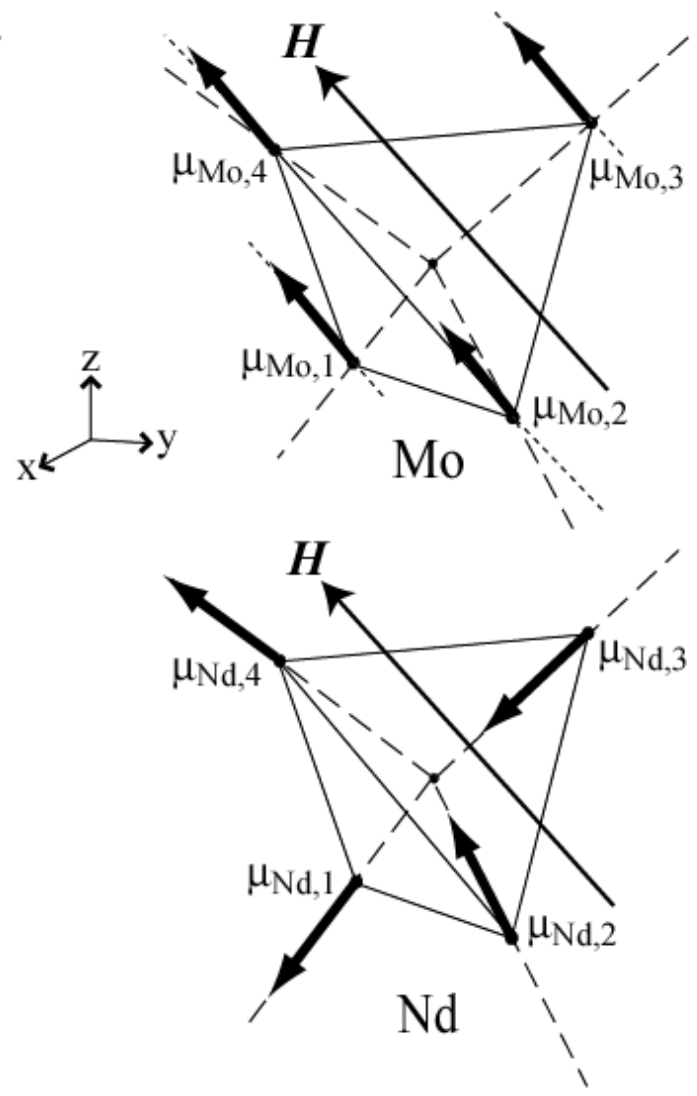


Fig. 4

(a) $H \rightarrow 0T$



(b) $H = 5.7T$



(c)

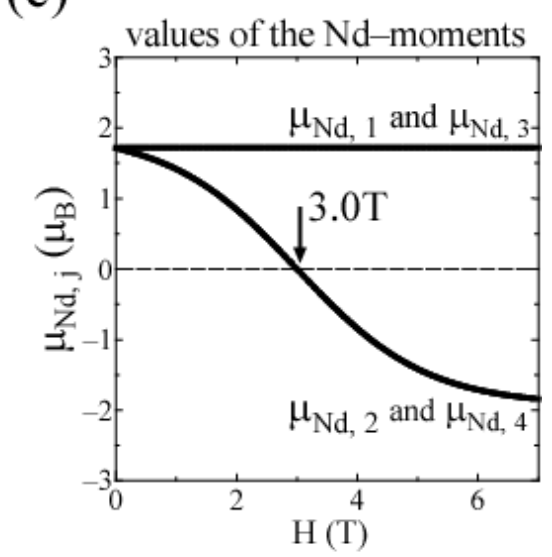


Fig. 5

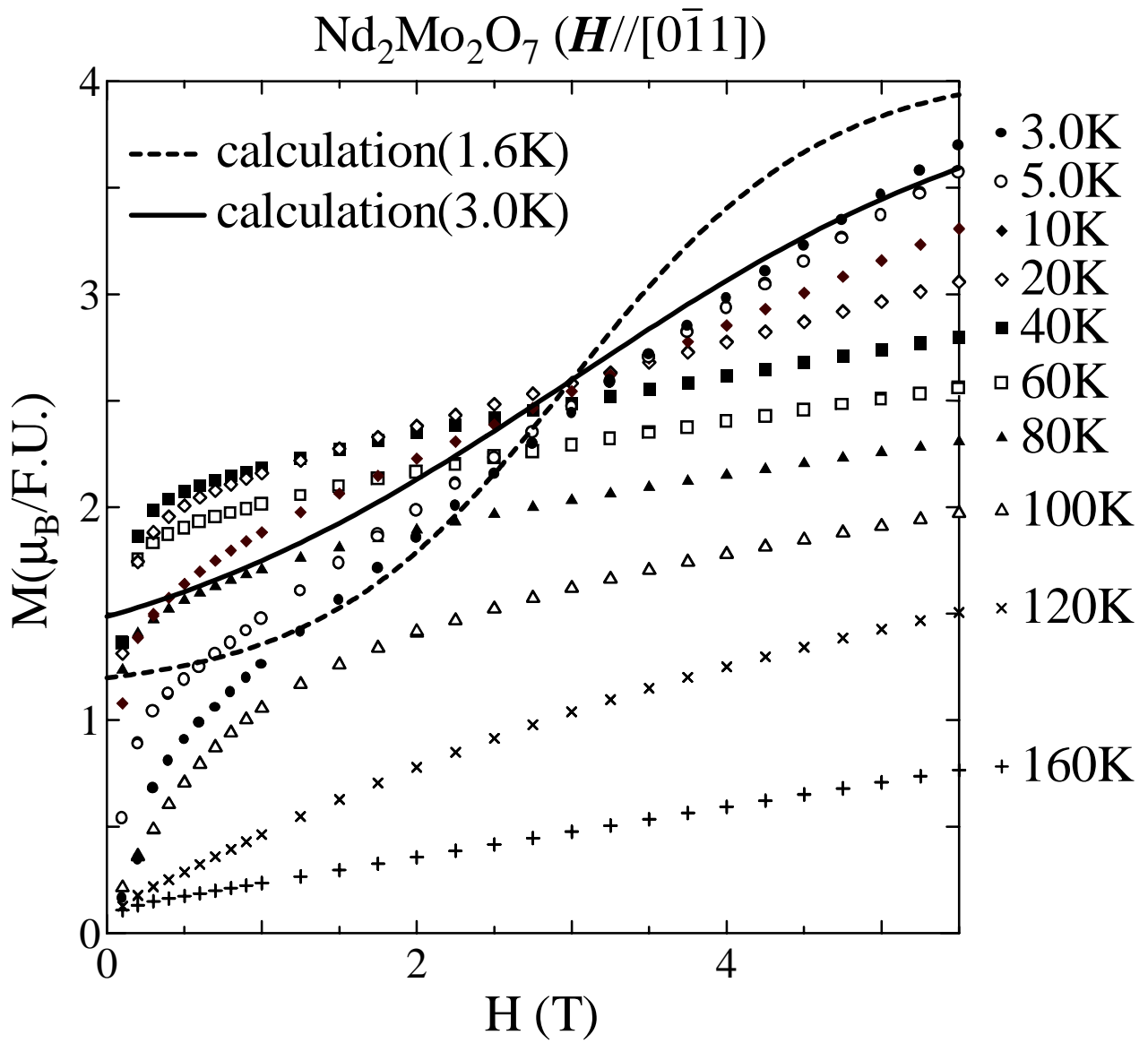


Fig. 6

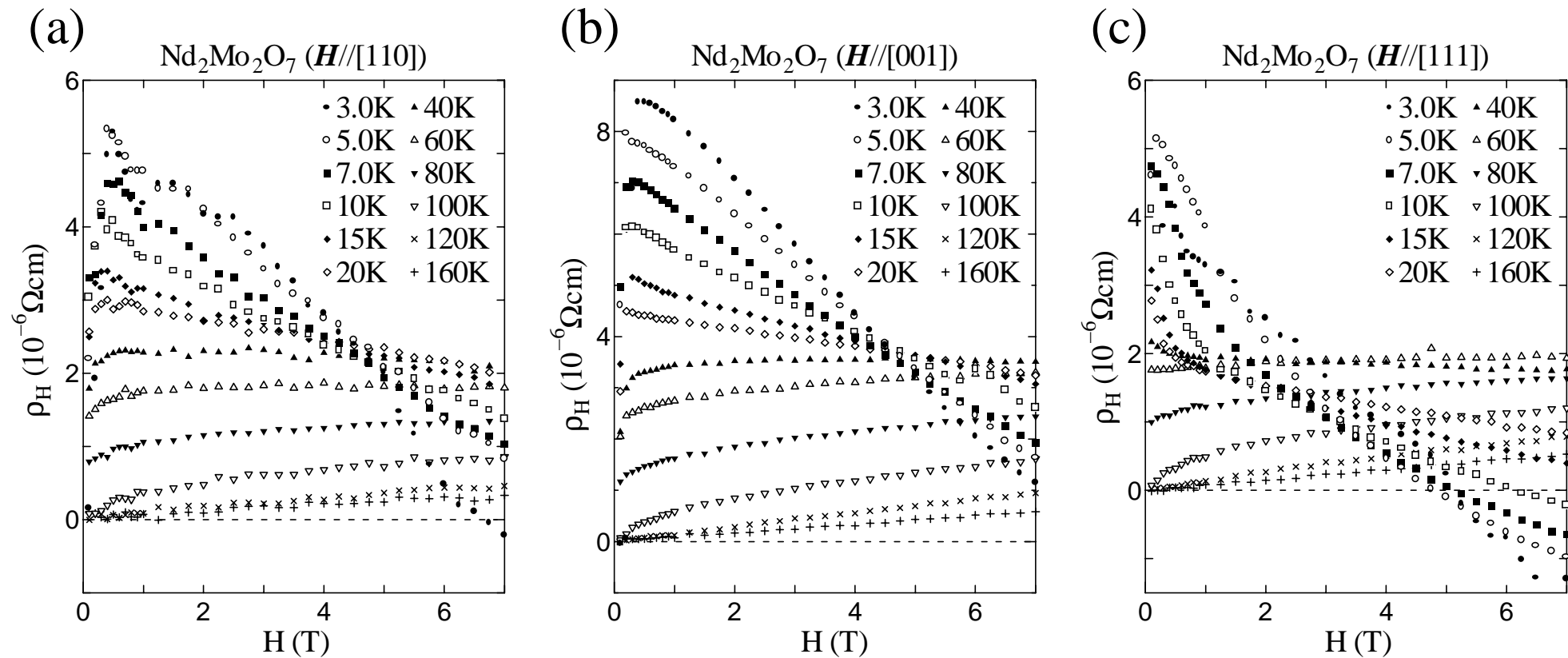


Fig. 7

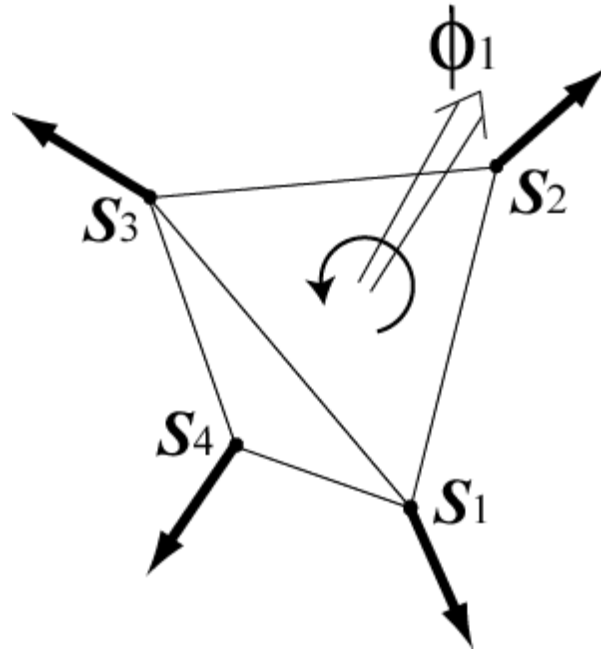


Fig. 8

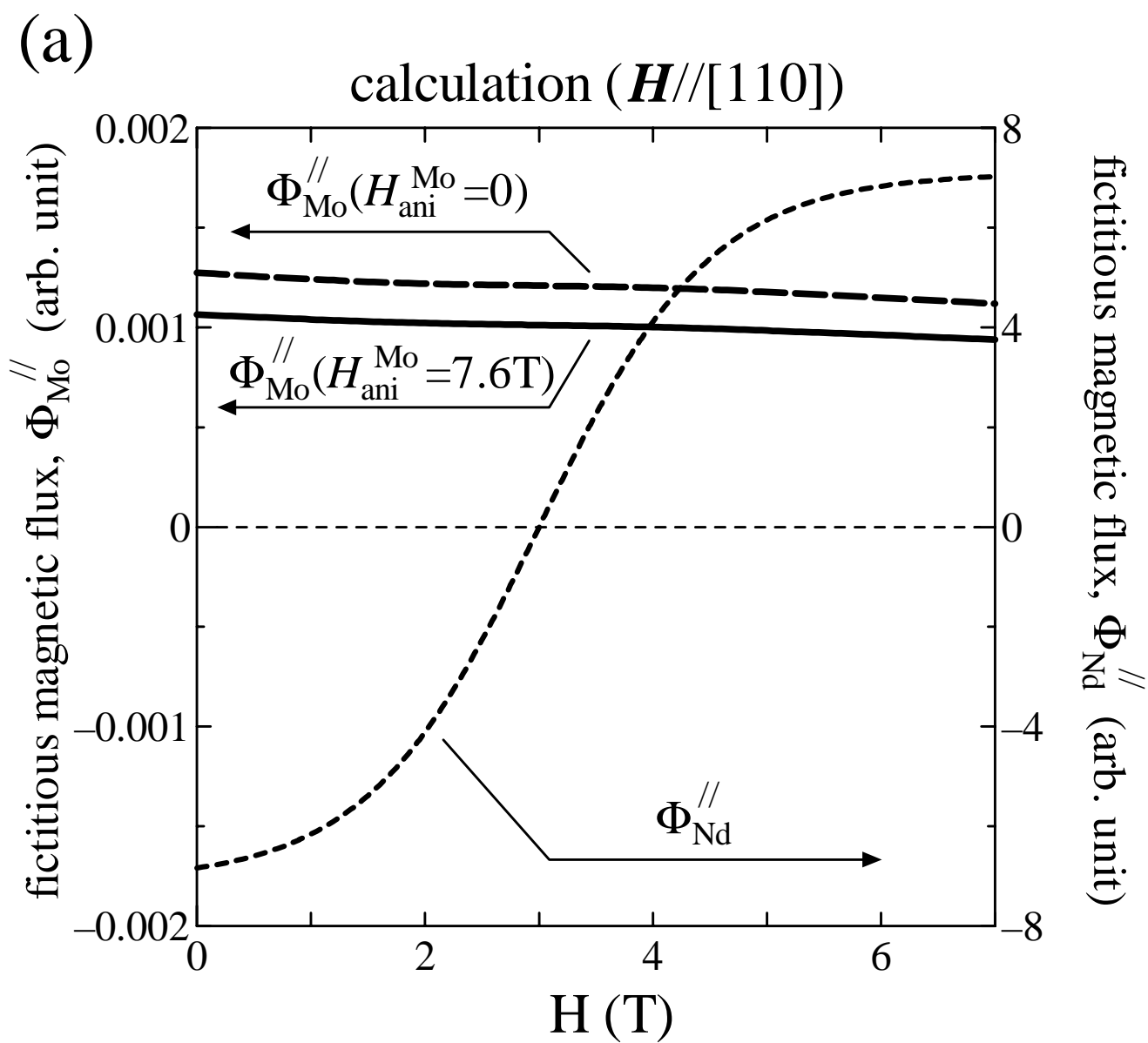


Fig. 9(a)

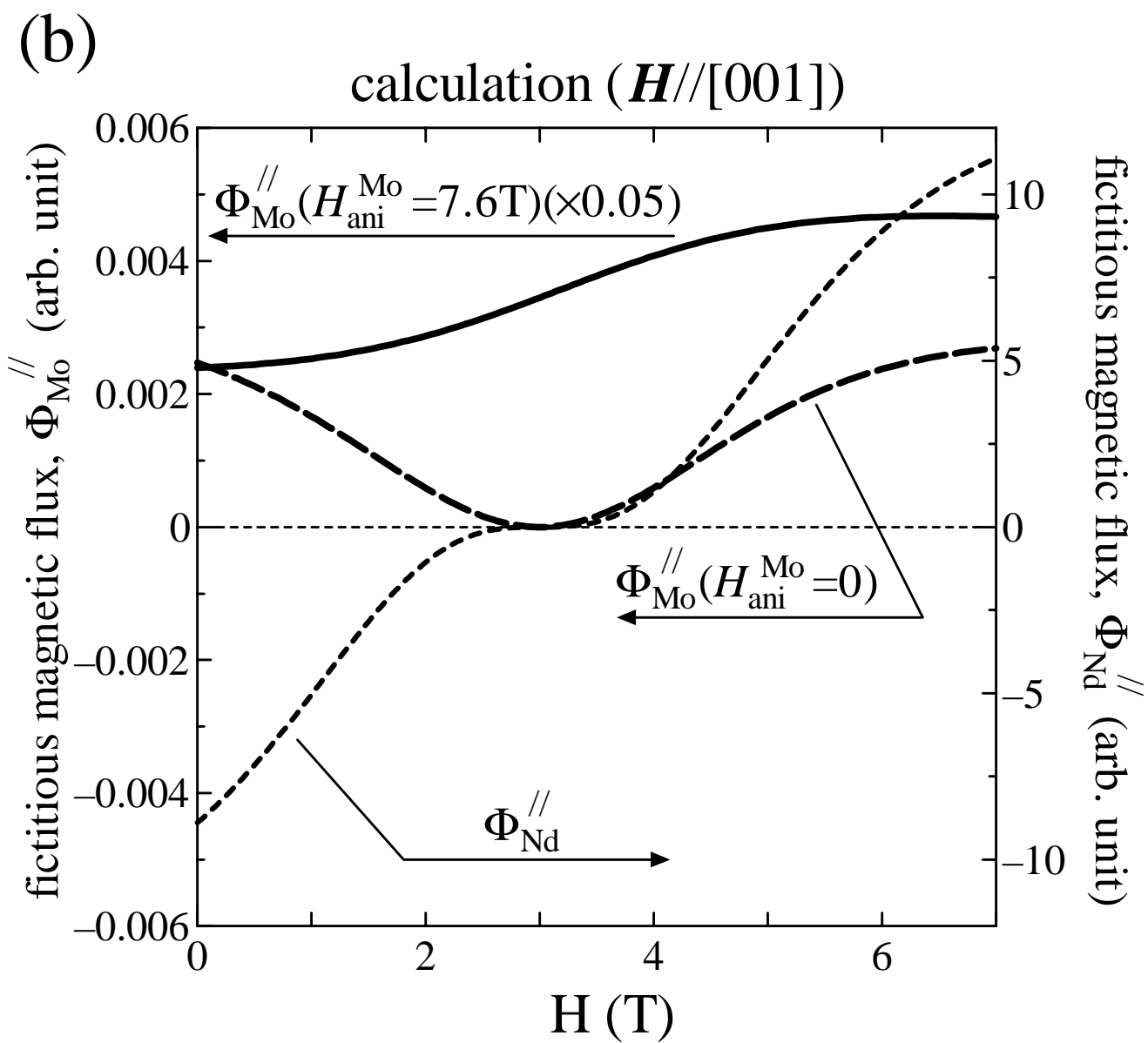


Fig. 9(b)

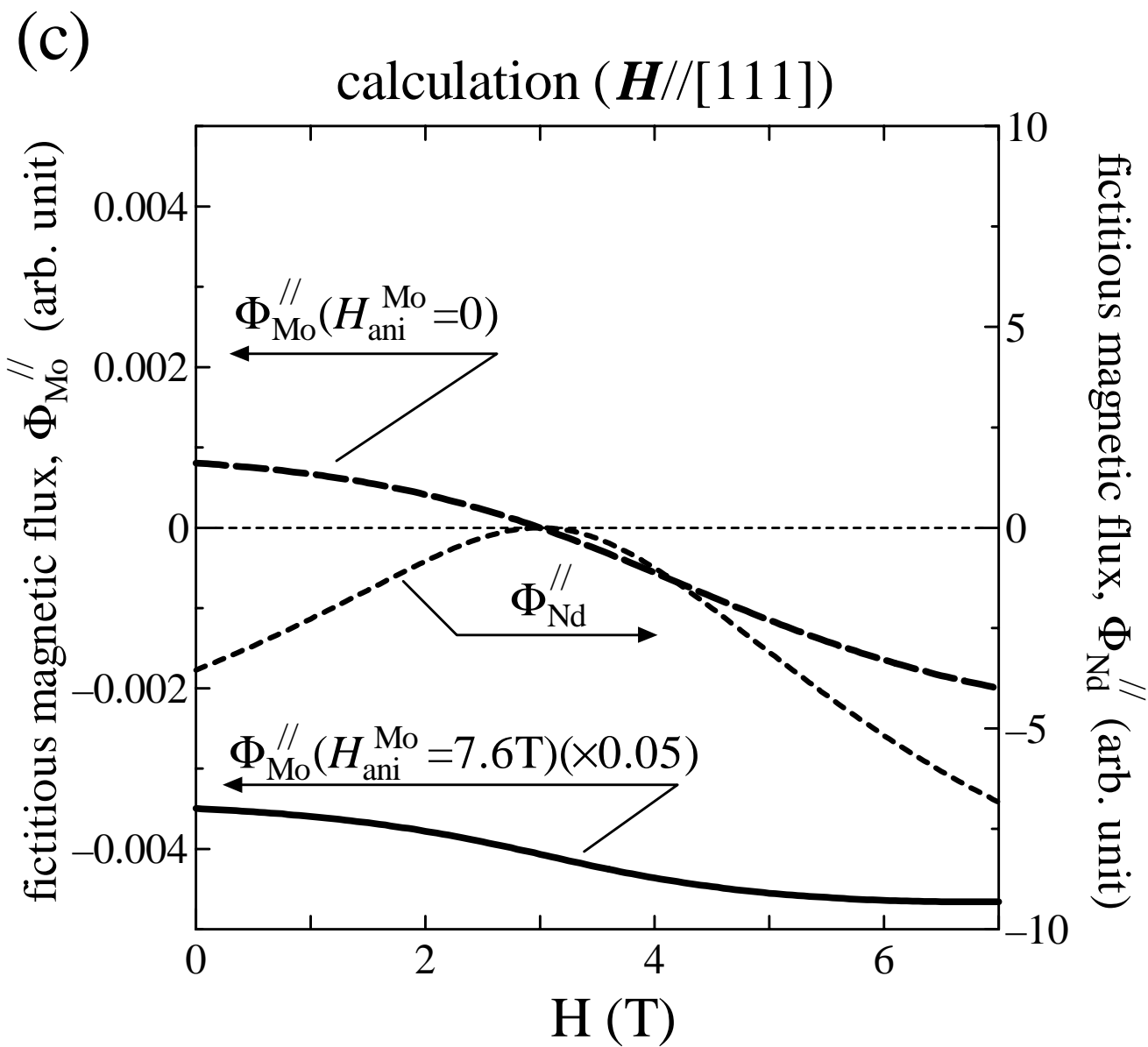


Fig. 9(c)

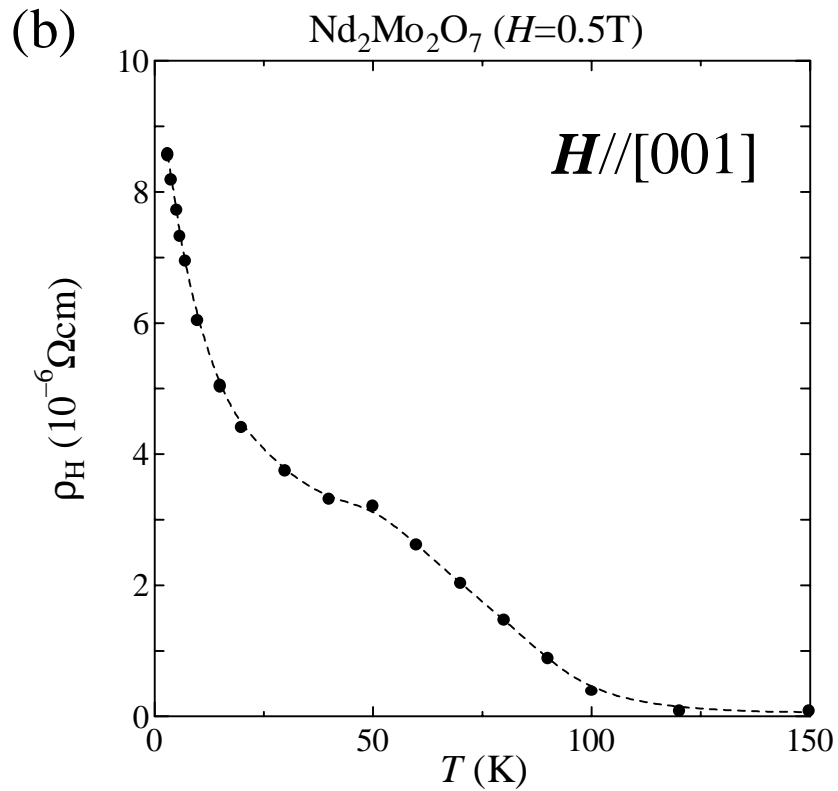
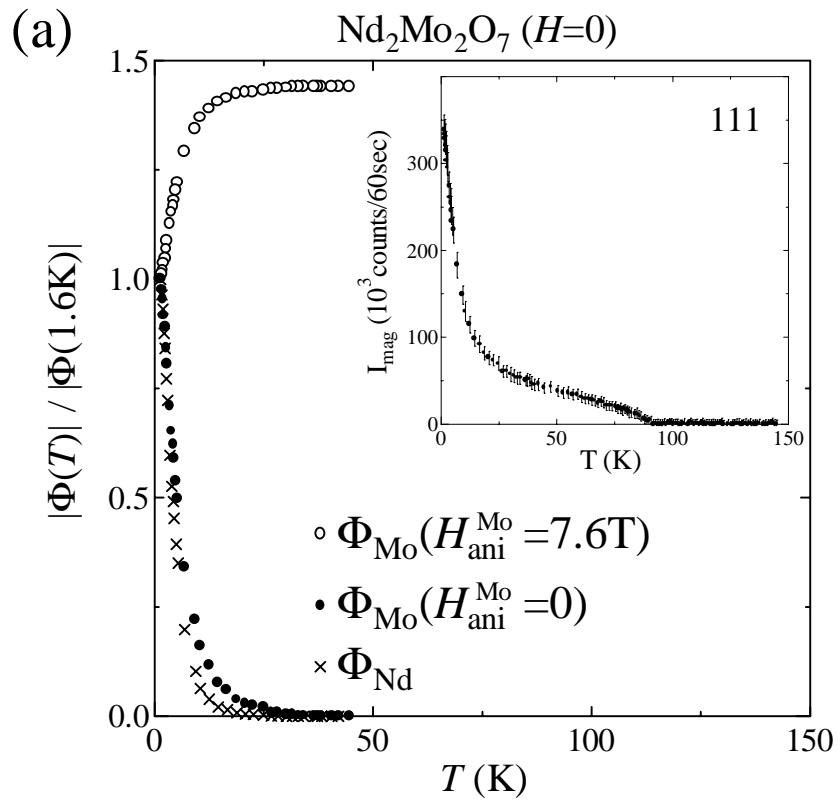


Fig. 10